arXiv:cond-mat/0507502v2 [cond-mat.mtrl-sci] 3 Dec 2005

Low frequency Rabi spectroscopy for a dissipative two-level system

Ya. S. Greenberg[1](*), E. Il'ichev[2] and A. Izmalkov[2]

[1] *Novosibirsk State Technical University, 20 K. Marx Ave., 630092 Novosibirsk, Russia*
[2] *Institute for Physical High Technology, P.O. Box 100239, D-07702 Jena, Germany*

PACS. 03.65.Yz – Decoherence; open systems; quantum statistical methods.
PACS. 85.35.Be – Quantum well devices.
PACS. 85.35.Ds – Quantum interference devices.

Abstract. –

We have analyzed the interaction of a dissipative two level quantum system with high and low frequency excitation. The system is continuously and simultaneously irradiated by these two waves. If the frequency of the first signal is close to the level separation the response of the system exhibits undamped low frequency oscillations whose amplitude has a clear resonance at the Rabi frequency with the width being dependent on the damping rates of the system. The method can be useful for low frequency Rabi spectroscopy in various physical systems which are described by a two level Hamiltonian, such as nuclei spins in NMR, double well quantum dots, superconducting flux and charge qubits, etc. As the examples, the application of the method to a nuclear spin and to the readout of a flux qubit are briefly discussed.

It is well known that under resonant irradiation a quantum two level system (TLS) can undergo coherent (Rabi) oscillations. The frequency of these oscillations is proportional to the amplitude of the resonant field [1] and is much lower than the gap frequency of TLS. The effect is widely used in molecular beam spectroscopy [2], and in quantum optics [3].

During the last several years it has been proven experimentally that Rabi spectroscopy can serve as a valuable tool for the determination of relaxation times in solid state quantum mechanical two-level systems, qubits, to be used for quantum information processing [4]. These systems normally are strongly coupled to the environment, which results in the fast damping of Rabi oscillations. It prevents the use of conventional continuous measurements schemes for their detection, though the special schemes for the detection of coherent oscillations through a weak continuous measurement of a TLS were proposed in [5–7]. That is why Rabi oscillations are measured with the pulse technique through the statistic of switching events of the occupation probability between two energy levels with excitation and read out being taken at the gap frequency of TLS, which normally, lies in GHz range [8–11]. The main drawback of this technique is that it requires sophisticated high frequency readout electronics.

In this work we propose a new experimental method for a Rabi spectroscopy of a TLS, when readout electronics is continuously swept across the low (compare to the gap) Rabi

(*) E-mail: greenbergy@online.nsk.su

© EDP Sciences

resonance. The method is rather general and can be applied to a great variety of two level systems.

We consider a TLS which is irradiated continuously by two external sources. The first with a frequency ω_0, which is close to the energy gap between the two levels, excites the low frequency Rabi oscillations. Normally, Rabi oscillations are damped out with a rate, which is dependent on how strongly the system is coupled to the environment. However, if a second low frequency source is applied simultaneously to TLS it responds with persistent low frequency oscillations. The amplitude of these low frequency oscillations has a resonance at the Rabi frequency with the width being dependent on the damping rates of the system. Note, that this approach has a well known classical analog. Indeed, a damping rate of a classical oscillator can be easily obtained from its amplitude-frequency characteristics.

We start with a Hamiltonian of a driven TLS , which is subjected to both high and low frequency excitation:

$$H = \frac{\Delta}{2}\sigma_x + \frac{\varepsilon}{2}\sigma_z - \sigma_z F\cos\omega_0 t - \sigma_z G(t). \tag{1}$$

Here the first two terms describe an isolated TLS, which can model a great variety of situations in physics and chemistry: from a spin 1/2 particle in a magnetic field to superconducting flux and charge qubits [4], [12]. In order to be exact we consider the first two terms in (1) to describe a double-well system where only the ground states of the two wells are occupied, with Δ being the energy splitting of a symmetric ($\varepsilon = 0$) TLS due to quantum tunnelling between two wells. The quantity ε is the bias, the external energy parameter which makes the system asymmetric. The last two terms in (1) describe the interaction with external time-dependent high frequency, F, and low frequency, G fields which modulate the energy asymmetry between the two wells.

Hamiltonian (1) is written in the localized state basis, i.e., in the basis of states localized in each well. In terms of the eigenstates basis, which we denote by upper case subscripts for the Pauli matrices $\sigma_X, \sigma_Y, \sigma_Z$, Hamiltonian (1) reads:

$$\begin{aligned} H = &\left[\frac{\Delta}{\Delta_\varepsilon}F\cos\omega_0 t + \frac{\Delta}{\Delta_\varepsilon}G(t)\right]\sigma_X \\ &+ \left[\frac{\Delta_\varepsilon}{2} - \frac{\varepsilon}{\Delta_\varepsilon}F\cos\omega_0 t - \frac{\varepsilon}{\Delta_\varepsilon}G(t)\right]\sigma_Z, \end{aligned} \tag{2}$$

where $\Delta_\varepsilon = \sqrt{\Delta^2 + \varepsilon^2}$ is the gap between two energy states.

The inclusion of the dissipative environment in Hamiltonian (1), results in the Bloch-Redfield equations for the matrix operators σ_X, σ_Y, σ_Z, [13], [14]. For weak driving ($F \ll \Delta$), and for weak coupling of the TLS to the bath these equations can be approximated by Bloch-type equations [15]:

$$\langle\dot\sigma_Z\rangle = \left(2f\cos\omega_0 t + 2g(t)\right)\langle\sigma_Y\rangle - \Gamma_Z\left(\langle\sigma_Z\rangle - Z_0\right), \tag{3}$$

$$\begin{aligned} \langle\dot\sigma_Y\rangle = &-\left(2f\cos\omega_0 t + 2g(t)\right)\langle\sigma_Z\rangle \\ &+ \left[\frac{\Delta_\varepsilon}{\hbar} - \frac{2\varepsilon}{\Delta}f\cos\omega_0 t - \frac{2\varepsilon}{\Delta}g(t)\right]\langle\sigma_X\rangle - \Gamma\langle\sigma_Y\rangle, \end{aligned} \tag{4}$$

$$\langle\dot\sigma_X\rangle = -\left[\frac{\Delta_\varepsilon}{\hbar} - \frac{2\varepsilon}{\Delta}f\cos\omega_0 t - \frac{2\varepsilon}{\Delta}g(t)\right]\langle\sigma_Y\rangle - \Gamma\langle\sigma_X\rangle, \tag{5}$$

where $f = \Delta \mathrm{F}/\hbar\Delta_\varepsilon$, $g(t) = \Delta \mathrm{G(t)}/\hbar\Delta_\varepsilon$, and $Z_0 = -\tanh\left(\Delta_\varepsilon/k_BT\right)$ is the equilibrium polarization of the system in the absence of external excitation sources ($f = 0$, $g = 0$). The angled brackets in Eqs. (3), (4), and (5) denote the trace over reduced density matrix $\rho(t)$, which is obtained by tracing out all environment degrees of freedom: $\langle\sigma_X\rangle = Tr(\sigma_X\rho(t))$, etc. In order to simplify the problem we assume the relaxation, Γ_Z and dephasing, Γ, rates in (3)-(5) are time-independent, i.e. the rates are slowly varying functions on the scale of Rabi period which is of the order of $1/f$.

Assuming that a high frequency driving amplitude F is sufficiently small we write the desired solution of Eqs. (3), (4), and (5) as:

$$\langle\sigma_Z\rangle = Z(t), \tag{6}$$

$$\langle\sigma_Y\rangle = Y(t) + A(t)\cos(\omega_0 t) + B(t)\sin(\omega_0 t), \tag{7}$$

$$\langle\sigma_X\rangle = X(t) + C(t)\cos(\omega_0 t) + D(t)\sin(\omega_0 t), \tag{8}$$

where X, Y, Z, A, B, C, and D are slowly varying, as compared to the high frequency ω_0, quantities.

As is known, a two-level system resonantly irradiated with a high frequency undergoes a low frequency Rabi oscillations. However, if the external low frequency excitation, $G(t)$ is absent ($g = 0$), the Rabi oscillations are damped out. For this case we obtain at the degeneracy point ($\varepsilon = 0$) the following solution: $X = 0$, $Y = 0$, $C = B$, $D = -A$,

$$Z(t) = z^* + z_0 e^{-\Gamma_1 t} + e^{-\Gamma_2 t}\left(z_1\cos\omega_R t + z_2\sin\omega_R t\right), \tag{9}$$

$$A(t) = a^* + a_0 e^{-\Gamma_1 t} + e^{-\Gamma_2 t}\left(a_1\cos\omega_R t + a_2\sin\omega_R t\right), \tag{10}$$

$$B(t) = b^* + b_0 e^{-\Gamma_1 t} + e^{-\Gamma_2 t}\left(b_1\cos\omega_R t + b_2\sin\omega_R t\right), \tag{11}$$

where the relaxation rates, Γ_1, Γ_2, and the Rabi frequency ω_R are determined by the equation

$$(\lambda - i\Gamma)^2(\lambda - i\Gamma_Z) - (\lambda - i\Gamma)f^2 - (\lambda - i\Gamma_Z)\delta^2 = 0. \tag{12}$$

Here λ is the eigenvalue for the oscillation mode, e. g., $Z(t) \approx e^{i\lambda t}$. This cubic equation has simple analytic solutions only for two cases. Firstly, in the absence of a relaxation in Eqs. (3) - (5) ($\Gamma_Z = \Gamma = 0$) we obtain $\Gamma_1 = \Gamma_2 = 0$, $\omega_R = \sqrt{\delta^2 + f^2}$, where δ is the high frequency detuning parameter, $\delta = \omega_0 - \Delta_\varepsilon/\hbar$. Secondly, for $\delta = 0$ we obtain $\Gamma_1 = \Gamma$, $\Gamma_2 = (\Gamma + \Gamma_Z)/2$, $\omega_R = \sqrt{f^2 - (\Gamma - \Gamma_Z)^2/4}$. For the subsequent derivation we need only the quantities z^*, a^*, b^* which can be determined as the steady state solution of the equations (3), (4), and (5): $z^* = P_Z Z(0)$, $a^* = z^* f\Gamma/(\Gamma^2 + \delta^2)$, $b^* = z^* f\delta/(\Gamma^2 + \delta^2)$, where $P_Z = \frac{\Gamma_Z\left(\Gamma^2+\delta^2\right)}{\Gamma_Z(\Gamma^2+\delta^2)+f^2\Gamma}$.

The quantity $P_Z Z_0$ is the nonequilibrium polarization, i. e., the steady state difference of occupation probabilities between two energy levels in the case when the high frequency excitation is applied to the TLS. Therefore, in the absence of the low frequency excitation the Rabi oscillations decay with a rate Γ_2 given by Eq. (12). The main goal of our investigation is to obtain the persistent oscillations of the quantities $Z(t)$ (6), $Y(t)$ (7), $X(t)$ (8) which can be detected with low frequency (compared to the gap) electronic circuitry. In what follows we show that a low frequency signal applied to TLS can sustain the persistent low frequency oscillations of the above mentioned quantities. The amplitude of these oscillations has a clear

resonance at the Rabi frequency with the width of the resonance being dependent on the damping rates of the system.

The Eqs. (3), (4), and (5) are analized in the presence of a low frequency excitation $G(t)$. We insert Eqs. (6), (7), (8) into (3), (4), and (5), and in accordance with the ideology of rotating wave approximation retain only the low frequency terms. We consider the force G to be small, and therefore neglect the terms which are of second and higher order in G. In addition, we keep only the terms which oscillate within the bandwidth of the Rabi frequency and neglect the terms which are of the order of $\hbar f/\Delta_\varepsilon$, $\hbar\Gamma/\Delta_\varepsilon$, $\hbar\Gamma_Z/\Delta_\varepsilon$. Consequently we obtain the following set of equations for low frequency quantities:

$$\dot{Z} = fA - \Gamma_Z Z \tag{13}$$

$$\dot{Y} = \frac{\Delta_\varepsilon}{\hbar} X - \Gamma Y + 2gz^* - \frac{\varepsilon}{\Delta} fB \tag{14}$$

$$\dot{X} = -\frac{\Delta_\varepsilon}{\hbar} Y - \Gamma X + \frac{\varepsilon}{\Delta} fA \tag{15}$$

$$\begin{aligned} \ddot{A} + 2\Gamma\dot{A} + (\Omega_R^2 + \Gamma^2)A = \\ f\left(\Gamma_Z - \Gamma\right) Z - \Gamma\frac{2\varepsilon}{\Delta} g b^* - \delta\frac{2\varepsilon}{\Delta} g a^* - \frac{2\varepsilon}{\Delta}\dot{g} b^* \end{aligned} \tag{16}$$

$$\begin{aligned} \ddot{B} + 2\Gamma\dot{B} + \left(\delta^2 + \Gamma^2\right) B = \\ -\delta f Z + \Gamma\frac{2\varepsilon}{\Delta} g a^* - \delta\frac{2\varepsilon}{\Delta} g b^* + \frac{2\varepsilon}{\Delta}\dot{g} a^* \end{aligned} \tag{17}$$

From these equations we can obtain the Fourier components for the slowly varying quantities $A(\omega)$ and $B(\omega)$, and for the low frequency persistent response of the TLS to a small low frequency excitation, $\widetilde{Z}(\omega)$, $\widetilde{Y}(\omega)$, and $\widetilde{X}(\omega)$: $\widetilde{C}(\omega) = \widetilde{B}(\omega)$, $\widetilde{D}(\omega) = -\widetilde{A}(\omega)$,

$$\widetilde{Z}(\omega) = \widetilde{g}(\omega)\frac{2\varepsilon}{\Delta} f^2 P_Z Z_0 \frac{\delta}{\delta^2 + \Gamma^2}\frac{2\Gamma + i\omega}{s(\omega)}, \tag{18}$$

$$\widetilde{A}(\omega) = \widetilde{g}(\omega)\frac{2\varepsilon}{\Delta} f P_Z Z_0 \frac{\delta}{\delta^2 + \Gamma^2}\frac{(2\Gamma + i\omega)\left(i\omega + \Gamma_Z\right)}{s(\omega)}, \tag{19}$$

$$\widetilde{B}(\omega) = -\widetilde{g}(\omega)\frac{2\varepsilon}{\Delta} f P_Z Z_0 \frac{\delta}{\delta^2 + \Gamma^2}\frac{1}{\left(\delta^2 + (\Gamma + i\omega)^2\right)}\left\{\frac{f^2\delta\left(2\Gamma + i\omega\right)}{s(\omega)} - \frac{\delta^2 - \Gamma^2 - i\omega\Gamma}{\delta}\right\}, \tag{20}$$

$$\widetilde{Y}(\omega) = \frac{\hbar}{\Delta_\varepsilon}\frac{\varepsilon}{\Delta} f\widetilde{A}(\omega) + \left(\frac{\hbar}{\Delta_\varepsilon}\right)^2\left(2\widetilde{g}(\omega) P_Z Z_0 - \frac{\varepsilon}{\Delta} f\widetilde{B}(\omega)\right)\left(\Gamma + i\omega\right), \tag{21}$$

$$\widetilde{X}(\omega) = \left(\frac{\hbar}{\Delta_\varepsilon}\right)^2\frac{\varepsilon}{\Delta} f\widetilde{A}(\omega)\left(\Gamma + i\omega\right) - \frac{\hbar}{\Delta_\varepsilon}\left(2\widetilde{g}(\omega) P_Z Z_0 - \frac{\varepsilon}{\Delta} f\widetilde{B}(\omega)\right), \tag{22}$$

where $s(\omega) = (\Omega_R - \omega + i\Gamma)(\Omega_R + \omega - i\Gamma)(i\omega + \Gamma_Z) - f^2\left(\Gamma_Z - \Gamma\right)$; $\Omega_R = \sqrt{\delta^2 + f^2}$ is the Rabi frequency in the absence of the damping ($\Gamma_Z = \gamma = 0$). ([1])

([1])In above expressions we disregard the Fourier components of the damping terms (Eqs. (9), (10), (11)) since for the persistent signal $g(t)$ they are unimportant.

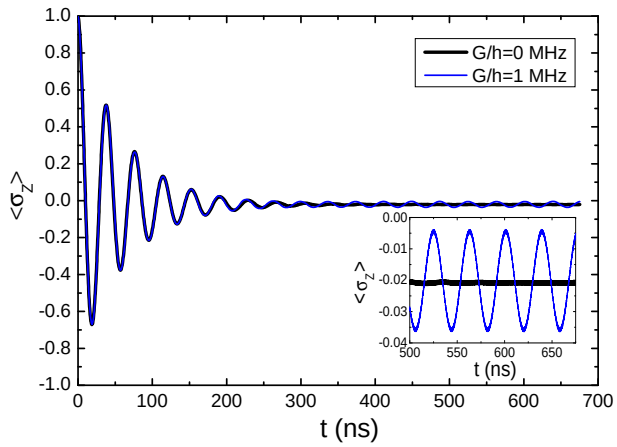

Fig. 1 – Time evolution of $< \sigma_z >$. (thick) G=0, (thin) $G/h = 1$ MHz. The insert shows the undamped oscillations of $< \sigma_z >$ at $G/h = 1$ MHz.

As can be concluded from these expressions the persistent low frequency oscillations of the spin components $Z(t)$, $X(t)$, $Y(t)$ appear as the response to the low frequency external force, $g(t)$, only in the presence of the high frequency excitation ($f \neq 0$). Exactly at resonance ($\delta = 0$) $\widetilde{A}(\omega) = 0$, and $\widetilde{Z}(\omega) = 0$, but $\widetilde{B}(\omega) \neq 0$. At this point the population of the two levels are equalized, and spin circularly rotates in the XY plane with frequency ω_0, with the center of the circle being precessed with the frequency ω of the low frequency external source.

As an example we show below the time evolution of the quantity $\langle \sigma_Z \rangle(t) = Z(t)$, obtained from the numerical solution of the equations (3), (4), and (5) where we take a low frequency excitations as $G(t) = Gcos(\omega_L t)$. The calculations have been performed with initial conditions $\langle \sigma_Z \rangle(0) = 1$, $\langle \sigma_X \rangle(0) = \langle \sigma_Y \rangle(0) = 0$ for the following set of the parameters: $F/h = 36$ MHz, $\Delta/h = 1$ GHz, $\Gamma/2\pi = 4$ MHz, $\Gamma_z/2\pi = 1$ MHz, $\epsilon/\Delta = 1$, $Z_0 = -1$, $\delta/2\pi = 6.366$ MHz, $\omega_L/\Omega_R = 1$. As is seen from Fig.1 in the absence of low frequency signal ($G = 0$) the oscillations are damped out, while if $G \neq 0$ the oscillations persist.

The Fourier spectra of these signals are shown on Fig.2 for different amplitudes of low frequency excitation. For $G = 0$ the Rabi frequency is positioned at approximately 26.2 MHz, which is close to $\Omega_R = 26.24$ MHz. With the increase of G the peak becomes higher. It is worth noting the appearance of the peak at the second harmonic of Rabi frequency. This peak is due to the contribution of the terms on the order of G^2 which we omitted in our theoretical analysis. The comparison of analytical and numerical resonance curves calculated for low frequency amplitude, $G/h = 1$ MHz and different dephasing rates, Γ are shown on Fig.3. The curves at the figure are the peak-to-peak amplitudes of oscillations of $Z(t)$ calculated from Eq. (18) with $\widetilde{g}(\omega) = g(\delta(\omega + \omega_L) + \delta(\omega - \omega_L))/2$, where $\delta(\omega)$ is Dirac delta function. The point symbols are found from numerical solution of Eqs. (3),(4),(5). The widths of the curves depend on Γ (see the insert) and the positions of the resonances coincide with the Rabi frequency. A good agreement between numerics and Eq. 18, as shown at Fig. 3, is observed only for relative small low frequency amplitude G/h, for which our linear response theory is valid.

The key point of the method we described above is that it allows for the detection of the high frequency response of a TLS at a frequency which is much less than the gap frequency. The low frequency dynamics of the quantities $\langle \sigma_X \rangle, \langle \sigma_Y \rangle, \langle \sigma_Z \rangle$ bears the information about

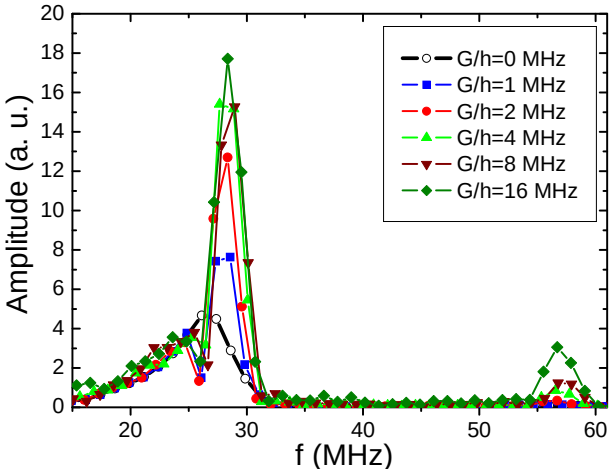

Fig. 2 – Fast Fourier transform of $< \sigma_z >$ at different amplitudes G/h of low-frequency field.

the relaxation, Γ_Z, and dephasing, Γ, rates.

The experimental realization of this method (the detection scheme) depends on the problem under investigation. For example, the method can easily be adapted for NMR. In this case the quantities $\langle \sigma_Z \rangle, \langle \sigma_X \rangle$, $\langle \sigma_Y \rangle$ are the longitudinal, M_Z, and the transversal polarizations of the sample, M_X, and M_Y. Indeed, from the comparison of the Hamiltonian (2) and the equations of motion (3), (4), (5) with those for nuclear spin ($H = -\vec{\mu}\vec{B}$, $d\vec{\mu}/dt = \gamma[\vec{\mu}\vec{B}]$, where γ is the gyromagnetic ratio), it is clear that the NMR case corresponds to the polarization of a sample with a field B_0 along the z axes with a high frequency excitation $B_1 cos(\omega_0 t)$ and a low frequency probe $G(t)$ being applied in the ZX plane at an angle θ to the z axis: $B_Z = B_0 + cos\theta(B_1 cos(\omega_0 t) + G(t))$, $B_X = -sin\theta(B_1 cos(\omega_0 t) + G(t))$, $B_Y = 0$. This anal-

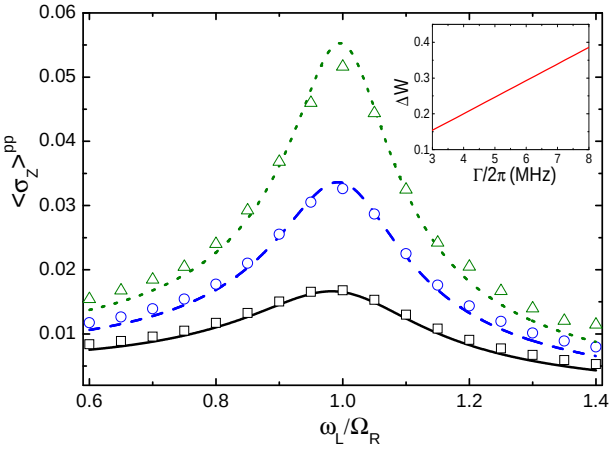

Fig. 3 – Peak-to-peak amplitude of $< \sigma_z >^{pp}$ undamped harmonic signal at $t \approx 700$ ns vs ω_L/Ω_R. $G/h = 1$ MHz, $\Gamma_Z/2\pi = 1$ MHz, (solid curve) $\Gamma/2\pi = 6$ MHz, (dashed curve) $\Gamma/2\pi = 4$ MHz, (dotted curve) $\Gamma/2\pi = 3$ MHz. The curves and the width of resonance, ΔW at $1/\sqrt{2}$ level (see the insert) are calculated from Eq. (18); the symbols are found from numerical solution of Eqs. (3),(4),(5).

ogy allows for the direct application of Eqs. (18)-(22) to the nuclear spin with the following substitutions: $\Delta_\varepsilon = \gamma\hbar B_0$, $\varepsilon/\Delta_\varepsilon = cos\theta$, $\Delta/\Delta_\varepsilon = sin\theta$, $f = \gamma B_1 sin\theta$, $g(\omega) = \gamma G(\omega) sin\theta$, $\varepsilon/\Delta = \cot\theta$, $Z_0 = M_0$ - the equilibrium magnetization of a sample. In NMR all low frequency components of the magnetization, $\widetilde{Z}(\omega)$ (18), $\widetilde{Y}(\omega)$ (21), $\widetilde{X}(\omega)$ (22), and their combinations are accessible for the measurements.

Our method can be directly applied to a persistent current qubit, which is a superconducting loop interrupted by three Josephson junctions [16], [17]. For these qubits the successful experimental implementation of low frequency readout electronics has been demonstrated [18–20]. The average current in the qubit loop is proportional to the low frequency part of the quantity $\langle\sigma_Z\rangle(t)$, which is directly connected to the probabilities of occupation of the ground, $P_-(t)$, and the excited, $P_+(t)$ states: $\langle\sigma_Z\rangle(t)$=$P_-(t)$-$P_+(t)$. Therefore, this current can be detected through the variation of its magnetic flux either by a DC SQUID [21] or by a high quality resonant tank circuit inductively coupled to the qubit [18–20].

In conclusion, we proposed a method to study the Rabi oscillations in a dissipative TLS by irradiating it simultaneously with high, resonant, and low frequency. The low frequency response of a system has a clear resonance at the Rabi frequency with the resonance width being dependent on the damping rates. Therefore, the method allows for the experimental determination, in the low frequency domain, of the relaxation and dephasing rates of dissipative two-level systems.

* * *

We are grateful to D. Averin, M. Grajcar, A. Korotkov, A. Shnirman, A. Smirnov, A. Zagoskin, A. Maassen van den Brink, W. Krech and V. Shnyrkov for fruitful discussions.

The authors acknowledge the support from D-Wave Systems. Ya. G. acknowledges partial support by the INTAS grant 2001-0809. E. I. thanks the EU for support through the RSFQubit project.

REFERENCES

[1] I. I. Rabi, Phys. Rev. **51**, 652 (1937).
[2] Atomic and Molecular Beams: The State of The Art 2000, (Roger Compargue, ed.) Springer Verlag Telos, 2001.
[3] J. M. Raimond, M. Brune, and S. Haroche, Rev. Mod. Phys. **73**, 565 (2001).
[4] Y. Makhlin, G. Schon, and A. Shnirman, Rev. Mod. Phys. **73**, 357 (2001).
[5] D. V. Averin, cond-mat/0004364.
[6] A.N. Korotkov and D.V. Averin, Phys. Rev. B **64**, 165310 (2001).
[7] A.N. Korotkov, Phys. Rev. B **63**, 115403 (2001).
[8] Y. Nakamura, Yu.A. Pashkin, and J.S. Tsai., Phys. Rev. Lett. **87**, 246601 (2001).
[9] D. Vion et al., Science **296**, 886 (2002).
[10] J.M. Martinis, S. Nam, J. Aumentado, C. Urbina, Phys. Rev. Lett. **89**, 117901 (2002).
[11] I. Chiorescu et al., Science **299**, 1869 (2003).
[12] M. Grifoni, P. Hänggi, Phys. Repts. **304**, 229 (1998).
[13] F. Bloch, Phys. Rev.**105**, 1206 (1957); A. G. Redfield, IBM J. Res. Dev. **1**, 19 (1957).
[14] L. Hartmann, I. Goychuk, M. Grifoni, P. Hanggi, Phys. Rev. E **61**, R4687 (2000).
[15] S. Saito et al., cond-mat/0403425 (2004).
[16] J.E. Mooij et al., Science **285**, 1036 (1999).
[17] T. P. Orlando et al., Phys. Rev. B **60**, 15398 (1999).
[18] Ya. S. Greenberg et al., Phys. Rev B **66**, 214525 (2002).
[19] M. Grajcar et al., Phys. Rev. B **69**, 060501(R) (2004).

[20] E. Il'ichev et al., Phys. Rev. Lett. **91**, 097906 (2003).
[21] A. Lupascu, et al., Phys. Rev. Lett. **93**, 177006 (2004).